Since January 2020 Elsevier has created a COVID-19 resource centre with free information in English and Mandarin on the novel coronavirus COVID-19. The COVID-19 resource centre is hosted on Elsevier Connect, the company's public news and information website.

BBA - Biomembranes 1863 (2021) 183590

Contents lists available at ScienceDirect

BBA - Biomembranes

journal homepage: www.elsevier.com/locate/bbamem

Transport mechanisms of SARS-CoV-E viroporin in calcium solutions: Lipid-dependent Anomalous Mole Fraction Effect and regulation of pore conductance

Carmina Verdiá-Báguena, Vicente M. Aguilella, María Queralt-Martín *, Antonio Alcaraz *

Laboratory of Molecular Biophysics, Department of Physics, University Jaume I, 12071 Castellón, Spain

ARTICLE INFO

Keywords:
Ion channel
Viroporin
Transport mechanisms
Electrophysiology
Calcium regulation
Lipid-protein interactions

ABSTRACT

The envelope protein E of the SARS-CoV coronavirus is an archetype of viroporin. It is a small hydrophobic protein displaying ion channel activity that has proven highly relevant in virus-host interaction and virulence. Ion transport through E channel was shown to alter Ca^{2+} homeostasis in the cell and trigger inflammation processes. Here, we study transport properties of the E viroporin in mixed solutions of potassium and calcium chloride that contain a fixed total concentration (mole fraction experiments). The channel is reconstituted in planar membranes of different lipid compositions, including a lipid mixture that mimics the endoplasmic reticulum-Golgi intermediate compartment (ERGIC) membrane where the virus localizes within the cell. We find that the E ion conductance changes non-monotonically with the total ionic concentration displaying an Anomalous Mole Fraction Effect (AMFE) only when charged lipids are present in the membrane. We also observe that E channel insertion in ERGIC-mimic membranes – including lipid with intrinsic negative curvature – enhances ion permeation at physiological concentrations of pure $CaCl_2$ or KCl solutions, with a preferential transport of Ca^{2+} in mixed KCl-$CaCl_2$ solutions. Altogether, our findings demonstrate that the presence of calcium modulates the transport properties of the E channel by interacting preferentially with charged lipids through different mechanisms including direct Coulombic interactions and possibly inducing changes in membrane morphology.

1. Introduction

The Covid-19 pandemic has sparked intense research into the structure of the SARS-CoV-2 coronavirus aimed to understand its mechanism of infection and hamper its virulence [1–3]. The SARS-CoV-2 RNA genome encodes several membrane proteins, one of which, the envelope protein E, is a small hydrophobic protein with ion channel activity localized at the endoplasmic reticulum-Golgi intermediate compartment (ERGIC). Importantly, the E protein of SARS-CoV-2 shares a high degree of similarity with the severe acute respiratory syndrome coronavirus (SARS-CoV) E protein studied here and their transmembrane domains – responsible for the ion channel activity – have identical amino acid sequences [1,2,4]. In addition, recent in silico studies predict analogous ion channel activity of both proteins [1]. Viroporins have been associated to viral replication and pathogenesis [5]. However, only recently the mechanism by which the SARS-CoV-E protein ion activity is linked to pathogenesis was elucidated [6]. The imbalance in ion concentration within cell organelles caused by channel activity triggers an immune response and activates the inflammasome and the subsequent pro-inflammatory response and lung damage. In addition, the E channel activity improves virus production, confers virulence in vivo, and inhibitory mutations in the E amino acid sequence induce compensatory mutations in the virus to restore channel activity [6]. All in all, this evidence makes the E protein a target to find therapies for SARS associated diseases and live attenuated vaccines.

The E viroporin is a 75-amino acid-long protein with a transmembrane domain (TM) of ~30 residues (8–38) (Fig. 1A). The 3D structure of E viroporin from SARS-CoV was solved using solid-state NMR spectroscopy in lipid micelles [7] (Fig. 1B) and the 3D structure of its homologue in SARS-CoV-2 was also very recently obtained using the same technique in ERGIC-mimetic lipid bilayers [2]. It was also reported that SARS-CoV E protein forms a Ca^{2+} permeable channel in ERGIC-mimetic lipid bilayers. E viroporin channel activity was found to alter Ca^{2+} homeostasis within cells and overstimulate inflammasomes leading to immunopathology [8]. The high calcium gradient concentration between the cytoplasm and ERGIC (100 nM in cytoplasm in

* Corresponding authors.
E-mail addresses: mqueralt@uji.es (M. Queralt-Martín), alcaraza@uji.es (A. Alcaraz).

https://doi.org/10.1016/j.bbamem.2021.183590
Received 10 December 2020; Received in revised form 4 February 2021; Accepted 6 February 2021
Available online 20 February 2021

contrast with 0.4 mM in ERGIC) points to a major role of calcium in different pathways during the viral cycle. It is known that regulation of intracellular calcium concentrations is essential for several cell functions [6]. The above preliminary study [8] aimed to prove the channel permeability and selectivity to Ca^{2+} ions. However, solutions of pure $CaCl_2$ were used, which is an ionic environment somewhat different from the multiionic one existing within the cell organelles involved in Ca^{2+} homeostasis. Here, we specifically address E viroporin permeability to calcium in the presence of another monovalent salt.

In previous investigations we showed that the membrane composition has an important impact on ionic transport through E channels, what lead us to hypothesize that E TMs assemble with lipid molecules to form some sort of proteolipidic pore structures [9–11] (Fig. 1C). The two abovementioned 3D structural models for E viroporin [2,7] agree in a pentameric organization of E TMs stabilized by lipids (see Fig. 1B), with small differences between the two models in the α-helices tilting and in the resulting pore size. Rearrangements between different conformations would likely involve lipid-protein interactions and require notable internal flexibility. Having this in mind, the lipid molecules could participate in the pore structure in different forms. In the so-called "barrel stave" pores the lipids are located only in the pore mouths while the hydrophilic regions of the protein are the ones forming the channel walls in transmembrane orientation (alamethicin seems to be the only peptide of this category) [12,13]. Alternatively, if the length of proteins does not match the hydrophobic length of the bilayer, arrangements in form of "toroidal" pores should appear involving either protein tilting or membrane deformation [12,14–17]. This could provoke that lipid head groups may be interspersed between the proteins as shown in Fig. 1C.

In this scenario, calcium could modulate the transport properties of the E channel by a number of different mechanisms, such as direct electrostatic interactions with protein residues and lipid molecules, generating hydrophobic effects or inducing membrane deformations, among many others [15,18]. The affinity of a membrane channel for a particular ionic species can be assessed in different ways, being reversal potential (the potential needed to obtain zero current under a concentration gradient) and subsequent calculations of permeability ratios the most usual by far [19–23]. Here, we focus on another type of experiment that resembles more the multiionic environment of the E channel activity. It consists in measuring channel conductance in the presence of a mixture of two different species whose individual concentration is changed while the total concentration is kept constant [19,24]. When conductance changes monotonically between the two endpoints corresponding to each pure electrolyte, it is inferred that the channel has no affinity for any of the considered ions that behave independently [19,24]. However, in several channels conductance vs mole fraction curves do not change monotonically but show a marked minimum, being the calcium channels particularly prolific in this sense [19,24–28]. Such non-monotonic behavior is known as Anomalous Mole Fraction Effect (AMFE) and it is considered a measure of preferential selectivity [24] because the presence of a second ion inhibits the conductance of the first one.

2. Materials and methods

2.1. Materials and protein synthesis

1,2-Diphytanoyl-sn-glycero-3-phosphocholine (DPhPC), 1,2-diphytanoyl-sn-glycero-3-phospho-L-serine (DPhPS), 1,2-dioleoyl-sn-glycero-3-phosphocholine (DOPC), 1,2-dioleoyl-sn-glycero-3-phosphoethanolamine (DOPE), and 1,2-dioleoyl-sn-glycero-3-phospho-L-serine (DOPS) were purchased from Avanti Polar Lipids (Alabaster, AL). Full-length SARS-CoV E protein was kindly provided by Dr. Jaume Torres and synthesized and purified as previously described [9].

2.2. Ion channel reconstitution and ionic current recording

Planar bilayers were formed by apposition of two monolayers prepared from a solution 5 mg/ml in pentane of pure DPhPC, pure DPhPS, or a mixture of DOPC, DOPS and DOPE at different ratios as indicated in the text. Lipids were added on ~100 μm diameter orifices in the 15 μm-thick Teflon partition that separated two identical chambers [29,30].

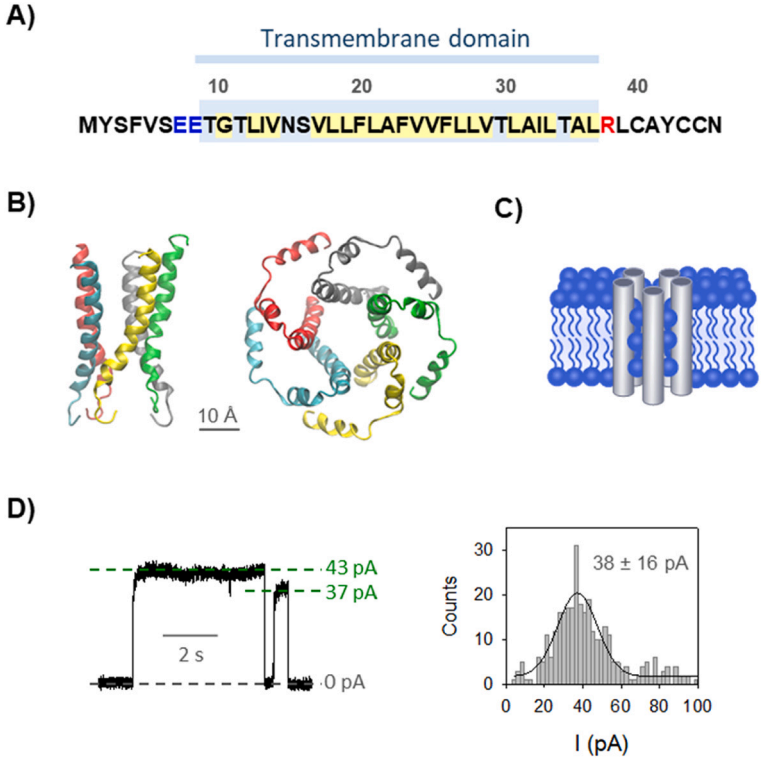

Fig. 1. SARS-CoV-E protein sequence, structure and channel formation. (A) Transmembrane domain (TM) sequence of E protein (accession number AYV99820). Blue and red letters represent acidic and basic residues, respectively, located at opposite ends of the TM. Hydrophobic amino acids within the TM are highlighted in yellow. (B) Top and side cartoon representations of E protein NMR pentameric structure of residues 8–65 (PDB code 5X29). Residues 40–65 are excluded in the side view for a better representation of the TM. Each monomer is shown in a different color. (C) Cartoon sketching a putative arrangement of five E protein monomers and lipid molecules to form a proteolipidic toroidal pore. (D) Representative E protein-induced channel current recording (left) and histogram of the current jump amplitudes (right) obtained in 1 M KCl at pH 6 with neutral PC membranes. Current recordings were digitally filtered at 1 kHz using a low-pass Bessel (8-pole) filter. Solid line in the histogram represents a single-Gaussian fitting with mean value and standard deviation as indicated. (For interpretation of the references to color in this figure legend, the reader is referred to the web version of this article.)

The orifices were pretreated with a 1% solution of hexadecane in pentane. Aqueous solutions of KCl were buffered with 5 mM HEPES and the pH was fixed at pH = 6 except otherwise noticed. All measurements were performed at room temperature (23 ± 1 °C). Ion channel insertion was achieved by adding 0.5–1 μl of a 300 μg/ml solution of synthetic protein in acetonitrile:isopropanol (40:60) to one side of the chamber (*cis* side). An electric potential was applied using Ag/AgCl electrodes in 2 M KCl, 1.5% agarose bridges assembled within standard 250 μl pipette tips. The potential was defined as positive when it was higher on the side of protein addition (*cis* side), whereas the *trans* side was set to ground. An Axopatch 200B amplifier (Molecular Devices, Sunnyvale, CA) in the voltage-clamp mode was used to measure the current and the applied potential. Data were filtered by an integrated low pass 8-pole Bessel filter at 10 kHz, saved with a sampling frequency of 50 kHz and analyzed using pClamp 10.7 software (Molecular Devices, Sunnyvale, CA). The chamber and the head stage were isolated from external noise sources with a double metal screen (Amuneal Manufacturing Corp., Philadelphia, PA).

The channel conductance was obtained from current measurements under an applied potential of +100 mV in symmetrical salt solutions. Current was calculated from a single-Gaussian fitting of the histogram of current jump amplitudes generated after addition of SARS-CoV E protein to the chamber. The standard deviation of the data corresponds to the sigma obtained from the Gaussian fit. Histograms contained at least 300 events from a minimum of 3 independent experiments. The reversal potential (the voltage corresponding to zero current) was measured on one or several channels under a salt concentration gradient of 500/50 mM KCl with or without a symmetrical addition of 15 mM $CaCl_2$. The measured value was corrected by the liquid junction potential from Henderson's equation [31] to obtain the final reversal potential. Permeability ratios between K^+ and Cl^-, P_+/P_-, where calculated according to the Goldman–Hodgkin–Katz equation [19]. In experiments with $CaCl_2$, the presence of 15 mM $CaCl_2$ at both sides of the membrane was taken into account to calculate the permeability ratios.

3. Results and discussion

Here, we investigate the interaction between calcium and E-induced pores by analyzing elementary current jumps in different mixtures of KCl and $CaCl_2$ (as shown in Fig. 1D, left panel). Conductance values (G) correspond to the mean value obtained from a single-Gaussian fit of the current jump amplitudes (see Fig. 1D) divided over the applied potential (G = I/V). Fig. 2 displays the E channel conductance vs the mole fraction of $CaCl_2$ in mixed solutions of $CaCl_2$ and KCl in negatively charged DPhPS (A, C) or neutral DPhPC (B, D) membranes and two total electrolyte concentrations, 50 mM and 1 M. Fig. 2A shows measurements performed in negatively charged PS membranes in 50 mM solutions. The curve in Fig. 2A shows a minimum at 0.15 Ca^{2+} mole fraction, which corresponds to 7 mM $CaCl_2$ and to a 43% reduction in the K^+ current relative to a pure KCl solution. As far as we know, this effect has not been described up to now in viroporins.

To probe whether membrane charge has an impact on the observed AMFE in Fig. 2A, we carried out similar experiments in neutral PC membranes. We found in this case that channel conductance seems to decrease monotonically with Ca^{2+} mole fraction (Fig. 2B). Even though data error bars are too large to be categorical, the trend shows no conclusive evidence on AMFE unlike that observed in Fig. 2A. The conventional explanation of AMFE points to the correlated movement of ions in a single file fashion [19] characteristic of very narrow channels like gramicidin A [32]. However, E channel unitary conductance is similar to another multiionic proteolipidic pore, alamethicin, in its lowest conductance state [9,33–35], which implies that it allows the

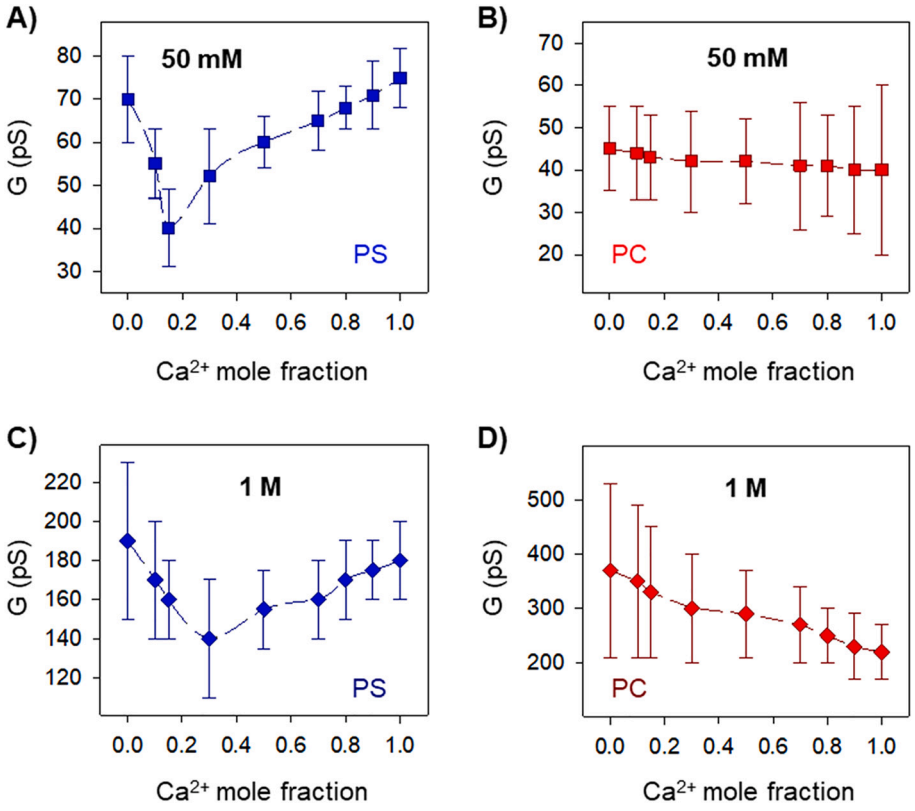

Fig. 2. SARS-CoV-E protein channels mole fraction experiments in mixed solutions of KCl and $CaCl_2$. Channel conductance as a function of Ca^{2+} mole fraction obtained at low (A, B) and high (C, D) total salt concentration in charged DPhPS (A, C) or neutral DPhPC (B, D) membranes. Channel conductance is measured at +100 mV applied potential. Here and elsewhere, each data point is calculated from a single-Gaussian fitting of the histogram of current jump amplitudes as shown in Fig. 1D.

transport of fully hydrated ions, water and small molecules [22]. Since single-file transport of dehydrated ions seems highly improbable in multi-ionic pores such as synthetic nanopores where AMFE has already been reported [25], it has been suggested that AMFE may appear also because of localized, ion-specific binding within the pore [25]. According to this explanation, in the presence of different permeant electrolytes, one of the ionic species binds tighter within the channel, excluding the other from the adjacent region. This creates a depletion zone that results in a decrease of channel conductance, given that the conductance for each ion is mostly determined by the region where it is present in the lowest concentration [36]. Thus, the reported AMFE (discernible in Fig. 2A and C despite the large error bars, but not visible in Fig. 2B and D) points to a preferential interaction of Ca^{2+} over K^+ ions in localized sites within the E proteolipidic channel.

The observation of AMFE only when the E viroporin is reconstituted in negatively charged membranes hints at the fact that Ca^{2+} ions interact preferably with lipid charges rather than with the acidic residues of the E protein TM. One distinctive trait of calcium-membrane interactions reported in GUVs is that increasing concentration of monovalent cations affects the binding affinity of Ca^{2+} [15]. To explore this effect in the E viroporin, we performed AMFE experiments in concentrated solutions. Fig. 2C and D display the change in conductance vs Ca^{2+} mole fraction when the total salt concentration is 1 M. Similar to what is shown in Fig. 2A–B for 50 mM solutions, AMFE is observed in PS membranes (Fig. 2C), but not in neutral ones (Fig. 2D) in 1 M solutions. However, the lowest conductance appears at higher Ca^{2+} mole fraction than in the respective low-concentration experiment (0.3 in Fig. 2C versus 0.15 in Fig. 2A) and the reduction in K^+ current is also smaller (26% in Fig. 2C vs 43% in Fig. 2A). Thus, in agreement with experiments in GUVS, high salt concentration yields screening effects that reduce the binding affinity of Ca^{2+} to negatively charged phospholipids [15].

An alternative route to probe the role of membrane charge in the interaction of Ca^{2+} ions with the pore is to assess the effect of solution acidity on AMFE experiments. pH acidification causes a charge neutralization of both the lipid and protein residues within the pore that is reflected in the channel ionic selectivity, which changes from cationic at neutral pH to anionic at acidic pH [8,10]. This effect is quantified in Fig. 3A by means of the permeability ratio P_{K+}/P_{Cl-} in E pores as a function of pH for neutral (PC) and charged membranes (PS) in KCl solutions, and for charged membranes in KCl + $CaCl_2$ solutions (PS + $CaCl_2$). It is clearly seen that under very acidic conditions (pH 1.5) the channel selectivity in KCl is very similar in neutral and charged membranes ($P_{K+}/P_{Cl-} = 0.43 \pm 0.06$ and $P_{K+}/P_{Cl-} = 0.54 \pm 0.07$, respectively). Hence, at this acidic pH the negative charges of the PS lipid are titrated by protons, so the lipid barely influences channel selectivity. To test the existence of AMFE in these conditions, we performed channel conductance experiments for varying mixtures of $CaCl_2$ and KCl at pH 1.5 (total salt concentration of 50 mM) (Fig. 3B). The monotonic change of conductance with Ca^{2+} molar fraction demonstrates that there is no AMFE when membrane lipid charge is neutralized, confirming that lipid charges are largely responsible for the calcium binding within this proteolipidic channel. Furthermore, the interaction between Ca^{2+} ions and negative lipid charges explains why addition of millimolar $CaCl_2$ in selectivity experiments with PS membranes (Fig. 3A, grey squares) reduces the channel preference for cations, which becomes similar to that obtained with PC membranes. Interestingly, measurements of P_{K+}/P_{Cl-} in PS with and without Ca^{2+} ions (Fig. 3A, grey squares and blue triangles) almost overlap at pH 1.5 ($P_{K+}/P_{Cl-} = 0.55 \pm 0.07$ and $P_{K+}/P_{Cl-} = 0.54 \pm 0.07$, respectively), implying that the interaction between lipid charges and Ca^{2+} vanishes once the lipid is titrated. Still, an interaction of Ca^{2+} ions with the E protein residues cannot be completely excluded, given that there is a small pKa shift in the titration experiments between neutral PC and *neutralized* PS + $CaCl_2$ membranes.

Next, we consider the more physiologically relevant lipid mixture PC/PE/PS 3:1:1 (w/w), which mimics the phospholipid headgroup composition of ERGIC membranes, the environment where E protein is

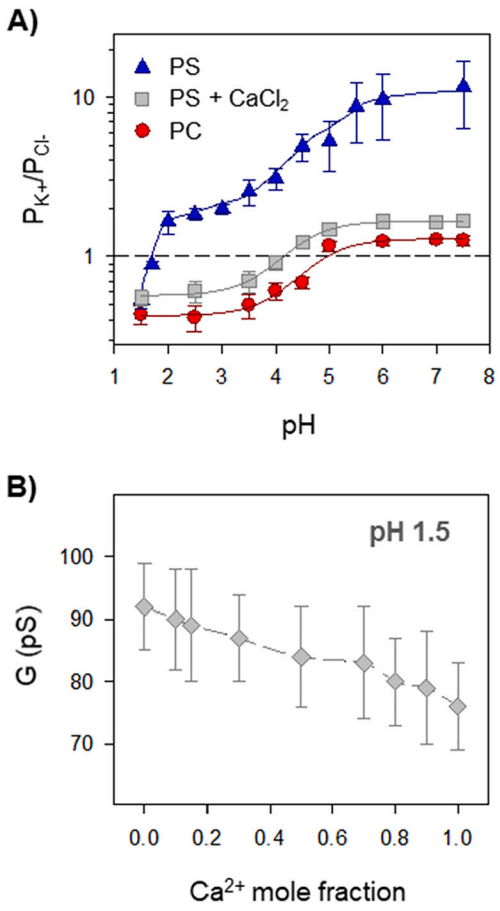

Fig. 3. Effect of lipid charge in the modulation of SARS-CoV-E protein channel function by Ca^{2+}. (A) Effect of pH on E protein permeability ratio, P_{K+}/P_{Cl-}, calculated from the corresponding reversal potential measurements under a salt concentration gradient of KCl 500 mM/50 mM in neutral (red circles) and in negatively charged membranes in the absence (blue triangles) or presence (grey squares) of symmetrical 15 mM $CaCl_2$. The dashed line at $P_{K+}/P_{Cl-} = 1$ corresponds to a non-selective ion channel. Error bars represent standard deviations from at least three independent experiments. Solid lines correspond to the best fit of the data to a standard sigmoidal dose–response curve with one (PC, PS + CaCl2) or two (PS) terms [8,10]. (B) Channel conductance vs Ca^{2+} mole fraction in mixtures of KCl and $CaCl_2$ with total concentration of 1 M in charged PS at pH 1.5.

localized [8]. Fig. 4A shows conductance vs Ca^{2+} mole fraction in ERGIC-like membranes (labelled as ERGIC) in 50 mM solutions of KCl + $CaCl_2$. Interestingly, AMFE appears in ERGIC membranes with a minimum at 0.4 mole fraction (corresponding to 20 mM Ca^{2+}) and a 44% reduction of K^+ current. To facilitate direct comparison, curves are shown together with measurements in PC and PS under the same conditions (50 mM). At each mole fraction, conductance is lower in neutral PC membranes than in charged PS or ERGIC membranes, even though conductance in PC is monotonic and it is not in PS and ERGIC. Of note, for solutions with predominant amount of KCl or $CaCl_2$ (mole fractions close to 0 and 1, respectively) the conductance in ERGIC membranes (with 20% charged lipid) is higher than in PS. Thus, an interesting observation is that in the native-like lipid composition E pores present an optimal combination of curvature and charge that yields maximum ion conduction in both pure KCl and $CaCl_2$. This implies that the intrinsic negative curvature of PE lipid (present in the ERGIC mixture with a 20% percentage) may be decisive to optimize the lipid packing, either inducing a membrane thinning or modifying the hydrophobic mismatch between the protein TM and the lipids [37]. Similar experiments performed at high electrolyte concentrations give a different scenario.

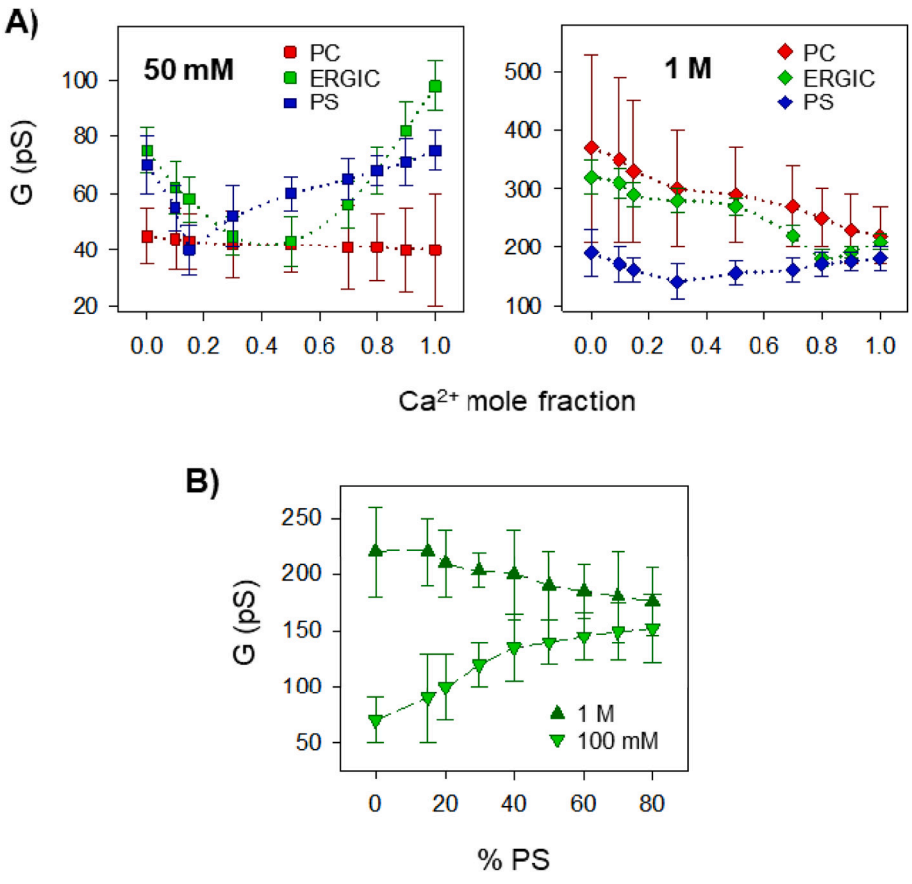

Fig. 4. Effect of non-lamellar lipid in the modulation of SARS-CoV-E protein channel function by Ca^{2+} ions. (A) Mole fraction experiments with mixtures of K^+ and Ca^{2+} obtained at low (left) and high (right) total salt concentrations in membranes formed by a lipid mixture of PC/PE/PS (3:1:1 w/w) mimicking the ERGIC membrane (green symbols). Experiments with pure neutral (red symbols) and pure negatively charged (blue symbols) lipid (Fig. 2) are shown for comparison. (B) Channel conductance as a function of the relative amount of PS in membranes formed with a fixed 20% of PE and a variable percentage of PC and PS, in high (1 M) and low (100 mM) $CaCl_2$ salt concentration. 0% PS corresponds to a membrane composition of PC:PE (8:2 w/w) while 80% PS corresponds to PS:PE (8:2 w/w).

Fig. 4B shows G vs Ca^{2+} mole fraction for PC, PS and ERGIC membranes at a total mixture concentration of 1 M. AMFE does exist in ERGIC membranes in these conditions, but it is barely visible. Importantly, the curve with lower conductance values is that of the fully charged membrane PS, being the neutral PC the one with higher measured conductance for all Ca^{2+} mole fractions. ERGIC (20% of PS) conductance is now in-between PC and PS, as could be expected if only the percentage of charged lipid is considered.

To examine in more detail the effect of lipid charge in ERGIC membranes, we performed channel conductance experiments in lipid mixtures with a fixed ratio of PE (20% w/w, as in ERGIC membranes) and a varying ratio of PC and PS (Fig. 4B). In line with the results in Fig. 4A, opposing trends are observed at low and high concentrations in Fig. 4B. At 100 mM $CaCl_2$, conductance increases with the relative amount of PS, which could be explained by the enhanced accumulation of ions available for conduction due to the increase of charge. However, in 1 M $CaCl_2$ channel conductance decreases with the increasing proportion of charged lipids, suggesting that the binding of cations to the lipid polar heads is so intense that it has an impact on ion mobility. The stronger the interaction, the slower the movement of cations through the channel [19].

Next, we examine how monovalent and divalent cations interact with E pores by focusing on pure electrolytes, either KCl or $CaCl_2$. Fig. 5A summarizes conductance experiments performed in 50 mM and 1 M solutions of KCl or $CaCl_2$, including now additional measurements in 1:1 PC:PS membranes. At low salt concentration, channel conductance in PC:PS (50% of charged lipid) falls in between pure PS and ERGIC (20% of charged lipid), demonstrating that the increased ion conduction observed in ERGIC is due to curvature effects (presence of PE) and not to a non-linear combination of PC and PS. Interestingly, at high concentration the channel conductance in ERGIC is halfway between PC and PC:PS 1:1, i.e. changing monotonically with the charged lipid content of the membrane and proving that curvature effects are no longer decisive.

Fig. 5A also shows that E channel conductance in KCl solutions is in general higher than in $CaCl_2$, which seems counterintuitive given that bulk solutions of $CaCl_2$ are more conductive than KCl ones (both for 50 mM and 1 M solutions). To explore this effect, we calculated the ratio between channel conductance in $CaCl_2$ and KCl for the same conditions of salt concentration and membrane composition. Results are presented in Fig. 5B, including the corresponding ratio between bulk conductivities as well. Fig. 5B shows that the ratio between $CaCl_2$ and KCl conductance is lower than that of bulk conductivities for all membrane compositions tested. This implies that the interaction with the E proteolipidic pore is in general stronger for Ca^{2+} than for K^+ ions, so that Ca^{2+} effective mobility is further reduced compared to bulk [10,22]. In addition, Fig. 5B demonstrates that the less charged the membrane, the lower the ratio between $CaCl_2$ and KCl conductance (except for ERGIC at 50 mM salt concentration). This corresponds to a larger difference in binding strength between K^+ and Ca^{2+} in PC than in PS membranes that causes a relatively higher decrease of Ca^{2+} than K^+ ion mobility in PC, compared to PS. This seems reasonable because, while K^+ ions interact very weakly with PC membranes, Ca^{2+} ions still bind to this neutral lipid [18,38], although to a lesser extent, given that no AMFE is observed in PC (Fig. 2). As commented before, the conductance ratio in ERGIC membranes at low salt concentration depicted in Fig. 5B is the only one that deviates from the general trend, pointing out again to the paramount importance of membrane curvature at physiologically low concentrations, where the $CaCl_2$/KCl conductance ratio approaches that of bulk conductivities.

To rationalize our findings, we may consider some general features of the interaction between cations and phospholipid membranes. The binding of Ca^{2+} to lipid membranes has been studied thoroughly [15,18,39,40], with a large scatter of measured calcium binding constants that may actually reflect a variety of different phenomena such as

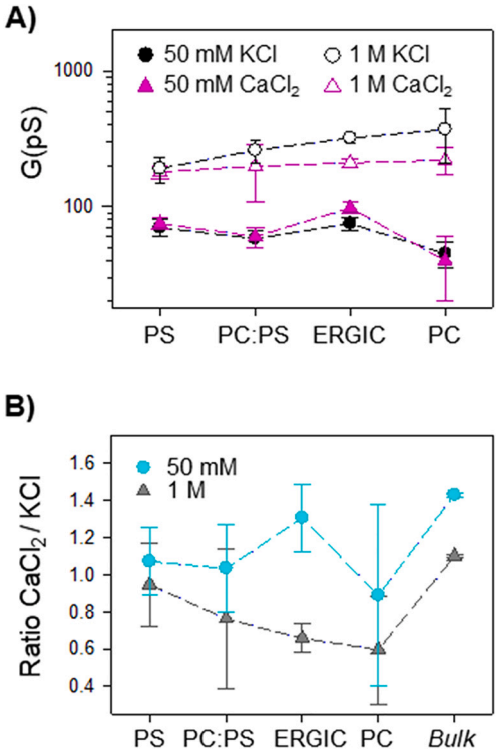

Fig. 5. Comparison of SARS-CoV-E protein channel conductance in different lipid mixtures and salt concentrations of pure KCl and $CaCl_2$ solutions. (A) E protein channel conductance measured in membranes of different lipid compositions at low (50 mM) and high (1 M) concentrations of KCl and $CaCl_2$ salts as labelled. (B) Ratio between measured conductance in $CaCl_2$ and KCl for different lipid compositions in 50 mM and 1 M solutions. *Bulk* denotes the corresponding solution conductivity ratio.

condensation effect of Ca^{2+} ions, phase separation of lipids or shape remodeling of membranes [15,18]. Ca^{2+} is thought to interact with lipid membranes spontaneously in an entropy-driven process [18] and occurs in a comparable fashion for negatively charged lipids and for zwitterionic lipids. The higher binding constants for negative lipids are potentially caused by the electrostatic enrichment of Ca^{2+} ions in the vicinity of the binding sites [18] and explain why we observe AMFE in charged PS but not in neutral PC (Fig. 2). Regarding the interaction between monovalent cations and lipid membranes, literature data also show considerable dispersion, but binding constants are smaller than for Ca^{2+} [38,39,41]. The interaction of monovalent cations with charged membranes is usually slightly stronger than with neutral ones, but the difference is not as marked as for divalent cations [41].

The most direct consequence of the binding process could be that bound cations might alter the dimensions of the pore eyelet via mutual repulsion or by other electrostatic interactions with the protein TM residues. However, more subtle mechanisms could operate as well. As mentioned before, notable changes in membrane morphology have been reported due to the presence of divalent Ca^{2+} but also for monovalent cations like K^+ or Na^+ [15]. Interestingly, those changes seem to operate in opposite directions. On the one side, experiments in GUVs show that interactions of Ca^{2+} with charged lipids induce negative curvature via membrane invaginations resulting in a decrease of the membrane area [15]. In contrast, similar experiments in the presence of Na^+ suggest that these cations could yield positive curvature [15] in agreement with simulations showing that the membrane curves away from monovalent cations to increase the separation between them [42]. Although it is unclear how those findings in GUVs could be directly used to interpret experiments in planar membranes, it is indisputable that the presence of cations near the lipid headgroups provokes different adaptation mechanisms [37]. The first one implies that bound cations could induce a change in the hydrophobic thickness of proteins and lipids. The second is based on membrane stretching that cause changes in lateral pressure profiles [37]. Hydrophobic interactions may be also an additional player to understand some of the counterintuitive findings relative to KCl and $CaCl_2$ conductance. According to the latest atomic structure of the SARS-CoV-2 E viroporin [2], the narrowest section of the E pore (~2 Å radius) is flanked by four layers of hydrophobic residues that would force ion dehydration to pass through. Given that Ca^{2+} hydration enthalpy is several times greater than K^+ one, this would be consistent with the higher conductance of E channel in KCl solutions than in $CaCl_2$ in low concentration solutions (Fig. 5B).

4. Conclusions

The hitherto accepted view of the E viroporin as a slightly cation selective multiionic pore with five transmembrane helices stabilized by the lipid and poor specific selectivity towards any particular ionic species seems insufficient to explain its calcium permeation properties in solutions where there are other monovalent ions. We have demonstrated that the E channel conductance in solutions of $CaCl_2$ + KCl does not change monotonically with the mole fraction of each salt but exhibits a minimum, an effect known in the literature as AMFE and characteristic of several calcium channels.

Our experiments suggest that the ionic transport properties of the SARS-CoV-E viroporin in solutions containing both monovalent and divalent cations are strongly dependent on the membrane lipid composition, the ratio between $CaCl_2$ and KCl concentrations, as well as on the total salt concentration. The influence of the membrane lipid composition has two aspects, probably intertwined: on the one hand the interaction of cations with negatively charged lipid polar heads; on the other hand, the effect of lipids with intrinsic negative curvature as DOPE on the conformation of the five E transmembrane helices. This is consistent with the reported effect of membrane environment on the protein helical conformation and the established proteolipidic character of the SARS-CoV-E viroporin.

Both monovalent and divalent cations interact strongly with negatively charged lipids yielding two main effects: an accumulation of ions due to Coulombic screening that enhances channel conductance at low concentration, and specific binding that becomes dominant at high concentration and induces relatively slower permeation. These two effects are clearly visible when comparing conductance in charged and neutral lipids: at low salt concentrations, conductance G(PC) < G(PS) because there is hardly any ion accumulation in neutral PC membranes. At high electrolyte concentration, G(PC) > G(PS) because the interaction between cations and neutral lipids is milder than with charged PS and has a more limited impact on ion permeation. As regards the comparison between Ca^{2+} and K^+ binding, we may conjecture that divalent cations have a higher affinity for lipids than monovalent ones. We believe this is the cause of the reported AMFE, which occurs at Ca^{2+} mole fractions lower than 0.5, consequently causing a larger difference between channel conductance and bulk conductivity as salt concentration increases. E channels reconstituted in ERGIC-mimic membranes display effects that cannot be easily attributed to the small lipid charge but are probably linked to a different protein-lipid arrangement induced by DOPE. At physiological $CaCl_2$ or KCl concentrations, these membranes enhance ion permeation in pure salts and optimize Ca^{2+} over K^+ transport in mixed KCl + $CaCl_2$ solutions. It is remarkable that these effects arise just in lipid bilayers resembling the natural environment of the E protein channel activity.

Altogether, this work provides novel insights on SARS-CoV E protein function and demonstrates that the presence of calcium modulates the transport properties of the E channel by interacting preferentially with charged lipids within the pore through different interaction mechanisms including direct Coulombic interactions and possibly changes in membrane morphology.

Declaration of competing interest

The authors declare the following financial interests/personal relationships which may be considered as potential competing interests: Antonio Alcaraz reports financial support was provided by Spanish Ministry of Science and Innovation. Maria Queralt-Martin reports financial support was provided by Spanish Ministry of Science and Innovation. Vicente M. Aguilella reports financial support was provided by Spanish Ministry of Science and Innovation.

Acknowledgments

Authors acknowledge financial support by the Spanish Agencia Estatal de Investigación (Projects 2019-108434GB-I00/AEI and IJC2018-035283-I/AEI), Generalitat Valenciana (Project AICO/2020/066), and Universitat Jaume I (Projects UJI-B2018-53 and UJI-A2020-21).

References

[1] Y. Cao, R. Yang, W. Wang, I. Lee, R. Zhang, W. Zhang, J. Sun, B. Xu, X. Meng, Computational study of the ion and water permeation and transport mechanisms of the SARS-CoV-2 pentameric E protein channel, Front. Mol. Biosci. 7 (2020) 1–14, https://doi.org/10.3389/fmolb.2020.565797.

[2] V.S. Mandala, M.J. McKay, A.A. Shcherbakov, A.J. Dregni, A. Kolocouris, M. Hong, Structure and drug binding of the SARS-CoV-2 envelope protein transmembrane domain in lipid bilayers, Nat. Struct. Mol. Biol. (2020), https://doi.org/10.1038/s41594-020-00536-8.

[3] Y. Yang, F. Peng, R. Wang, K. Guan, T. Jiang, G. Xu, J. Sun, C. Chang, The deadly coronaviruses: the 2003 SARS pandemic and the 2020 novel coronavirus epidemic in China, J. Autoimmun. 109 (2020) 102434, https://doi.org/10.1016/j.jaut.2020.102434.

[4] M. Sarkar, S. Saha, Structural insight into the role of novel SARSCoV-2 E protein: a potential target for vaccine development and other therapeutic strategies, PLoS One 15 (2020) 1–25, https://doi.org/10.1371/journal.pone.0237300.

[5] J.L. Nieto-Torres, C. Verdiá-Báguena, C. Castaño-Rodriguez, V.M. Aguilella, L. Enjuanes, Relevance of viroporin ion channel activity on viral replication and pathogenesis, Viruses 7 (2015) 3552–3573, https://doi.org/10.3390/v7072786.

[6] J.L. Nieto-Torres, M.L. DeDiego, C. Verdiá-Báguena, J.M. Jimenez-Guardeño, J. A. Regla-Nava, R. Fernandez-Delgado, C. Castaño-Rodriguez, A. Alcaraz, J. Torres, V.M. Aguilella, L. Enjuanes, Severe acute respiratory syndrome coronavirus envelope protein ion channel activity promotes virus fitness and pathogenesis, PLoS Pathog. 10 (2014), e1004077, https://doi.org/10.1371/journal.ppat.1004077.

[7] W. Surya, Y. Li, J. Torres, Structural model of the SARS coronavirus E channel in LMPG micelles, Biochim. Biophys. Acta Biomembr. 1860 (2018) 1309–1317, https://doi.org/10.1016/j.bbamem.2018.02.017.

[8] J.L. Nieto-Torres, C. Verdiá-Báguena, J.M. Jimenez-Guardeño, J.A. Regla-Nava, C. Castaño-Rodriguez, R. Fernandez-Delgado, J. Torres, V.M. Aguilella, L. Enjuanes, Severe acute respiratory syndrome coronavirus E protein transports calcium ions and activates the NLRP3 inflammasome, Virology 485 (2015) 330–339, https://doi.org/10.1016/j.virol.2015.08.010.

[9] C. Verdiá-Báguena, J.L. Nieto-Torres, A. Alcaraz, M.L. DeDiego, J. Torres, V. M. Aguilella, L. Enjuanes, Coronavirus E protein forms ion channels with functionally and structurally-involved membrane lipids, Virology 432 (2012) 485–494, https://doi.org/10.1016/j.virol.2012.07.005.

[10] C. Verdiá-Báguena, J.L. Nieto-Torres, A. Alcaraz, M.L. DeDiego, L. Enjuanes, V. M. Aguilella, Analysis of SARS-CoV E protein ion channel activity by tuning the protein and lipid charge, Biochim. Biophys. Acta Biomembr. 1828 (2013) 2026–2031, https://doi.org/10.1016/j.bbamem.2013.05.008.

[11] V.M. Aguilella, C. Verdiá-Báguena, A. Alcaraz, Lipid charge regulation of non-specific biological ion channels, Phys. Chem. Chem. Phys. 16 (2014) 3881–3893, https://doi.org/10.1039/c3cp54690j.

[12] G.C. Fadda, D. Lairez, G. Zalczer, Fluctuations of ionic current through lipid bilayers at the onset of peptide attacks and pore formation, Phys. Rev. Lett. 103 (2009) 1–4, https://doi.org/10.1103/PhysRevLett.103.180601.

[13] A. Grau-Campistany, E. Strandberg, P. Wadhwani, F. Rabanal, A.S. Ulrich, Extending the hydrophobic mismatch concept to amphiphilic membranolytic peptides, J. Phys. Chem. Lett. 7 (2016) 1116–1120, https://doi.org/10.1021/acs.jpclett.6b00136.

[14] A. Grau-Campistany, E. Strandberg, P. Wadhwani, J. Reichert, J. Bürck, F. Rabanal, A.S. Ulrich, Hydrophobic mismatch demonstrated for membranolytic peptides, and their use as molecular rulers to measure bilayer thickness in native cells, Sci. Rep. 5 (2015) 20–24, https://doi.org/10.1038/srep09388.

[15] Z.T. Graber, Z. Shi, T. Baumgart, Cations induce shape remodeling of negatively charged phospholipid membranes, Phys. Chem. Chem. Phys. 19 (2017) 15285–15295, https://doi.org/10.1039/c7cp00718c.

[16] E. Largo, M. Queralt-Martín, P. Carravilla, J.L. Nieva, A. Alcaraz, Single-molecule conformational dynamics of viroporin ion channels regulated by lipid-protein interactions, Bioelectrochemistry 137 (2021), 107641, https://doi.org/10.1016/j.bioelechem.2020.107641.

[17] E. Largo, C. Verdiá-Báguena, V.M. Aguilella, J.L. Nieva, A. Alcaraz, Ion channel activity of the CSFV p7 viroporin in surrogates of the ER lipid bilayer, Biochim. Biophys. Acta Biomembr. 1858 (2016) 30–37, https://doi.org/10.1016/j.bbamem.2015.10.007.

[18] C.G. Sinn, M. Antonietti, R. Dimova, Binding of calcium to phosphatidylcholine-phosphatidylserine membranes, Colloids Surf. A Physicochem. Eng. Asp. 282–283 (2006) 410–419, https://doi.org/10.1016/j.colsurfa.2005.10.014.

[19] B. Hille, Ion Channels of Excitable Membranes, Third ed., Sinauer Associates Inc, Sunderland, MA, 2001. http://www.sinauer.com/ion-channels-of-excitable-membranes.html#.UvDS-CVNRd8.mendeley.

[20] P. Ramírez, M. Aguilella-Arzo, A. Alcaraz, J. Cervera, V.M. Aguilella, Theoretical description of the ion transport across nanopores with titratable fixed charges: analogies between ion channels and synthetic pores, Cell Biochem. Biophys. 44 (2006) 287–312, https://doi.org/10.1385/CBB:44:2:287.

[21] M.L. López, E. García-Giménez, V.M. Aguilella, A. Alcaraz, Critical assessment of OmpF channel selectivity: merging information from different experimental protocols, J. Phys. Condens. Matter. 22 (2010), 454106, https://doi.org/10.1088/0953-8984/22/45/454106.

[22] V.M. Aguilella, M. Queralt-Martín, M. Aguilella-Arzo, A. Alcaraz, Insights on the permeability of wide protein channels: measurement and interpretation of ion selectivity, Integr. Biol. 3 (2011) 159–172, https://doi.org/10.1039/C0IB00048E.

[23] D. Gillespie, R. Eisenberg, Physical descriptions of experimental selectivity measurements in ion channels, Eur. Biophys. J. 31 (2002) 454–466, https://doi.org/10.1007/s00249-002-0239-x.

[24] D. Gillespie, D. Boda, The anomalous mole fraction effect in calcium channels: a measure of preferential selectivity, Biophys. J. 95 (2008) 2658–2672, https://doi.org/10.1529/biophysj.107.127977.

[25] D. Gillespie, D. Boda, Y. He, P. Apel, Z.S. Siwy, Synthetic nanopores as a test case for ion channel theories: the anomalous mole fraction effect without single filing, Biophys. J. 95 (2008) 609–619, https://doi.org/10.1529/biophysj.107.127985.

[26] W. Almers, E.W. McCleskey, Non-selective conductance in calcium channels of frog muscle: calcium selectivity in a single-file pore, J. Physiol. 353 (1984) 585–608, https://doi.org/10.1113/jphysiol.1984.sp015352.

[27] W. Almers, E.W. McCleskey, P.T. Palade, A non-selective cation conductance in frog muscle membrane blocked by micromolar external calcium ions, J. Physiol. 353 (1984) 565–583, https://doi.org/10.1113/jphysiol.1984.sp015351.

[28] D. Gillespie, Energetics of divalent selectivity in a calcium channel: the ryanodine receptor case study, Biophys. J. 94 (2008) 1169–1184, https://doi.org/10.1529/biophysj.107.116798.

[29] S.M. Bezrukov, I. Vodyanoy, Probing alamethicin channels with water-soluble polymers. Effect on conductance of channel states, Biophys. J. 64 (1993) 16–25, https://doi.org/10.1016/S0006-3495(93)81336-5.

[30] M. Montal, P. Mueller, Formation of bimolecular membranes from lipid monolayers and a study of their electrical properties, Proc. Natl. Acad. Sci. U. S. A. 69 (1972) 3561–3566, https://doi.org/10.1073/pnas.69.12.3561.

[31] A. Alcaraz, E.M. Nestorovich, M.L. López, E. García-Giménez, S.M. Bezrukov, V. M. Aguilella, Diffusion, exclusion, and specific binding in a large channel: a study of OmpF selectivity inversion, Biophys. J. 96 (2009) 56–66, https://doi.org/10.1016/j.bpj.2008.09.024.

[32] D.A. Kelkar, A. Chattopadhyay, The gramicidin ion channel: a model membrane protein, Biochim. Biophys. Acta Biomembr. 1768 (2007) 2011–2025, https://doi.org/10.1016/j.bbamem.2007.05.011.

[33] M. Queralt-Martín, M.L. López, M. Aguilella-Arzo, V.M. Aguilella, A. Alcaraz, Scaling behavior of ionic transport in membrane nanochannels, Nano Lett. 18 (2018) 6604–6610, https://doi.org/10.1021/acs.nanolett.8b03235.

[34] V.M. Aguilella, S.M. Bezrukov, V.M. Aguilella, Alamethicin channel conductance modified by lipid charge, Eur. Biophys. J. 30 (2001) 233–241, https://doi.org/10.1007/s002490100145.

[35] G.A. Woolley, Channel-forming activity of alamethicin: effects of covalent tethering, Chem. Biodivers. 4 (2007) 1323–1337, https://doi.org/10.1002/cbdv.200790113.

[36] W. Nonner, D.P. Chen, B. Eisenberg, Anomalous mole fraction effect, electrostatics, and binding in ionic channels, Biophys. J. 74 (1998) 2327–2334, https://doi.org/10.1016/S0006-3495(98)77942-1.

[37] L. Conrard, D. Tyteca, Regulation of Membrane Calcium Transport Proteins by the Surrounding Lipid Environment, 2019, https://doi.org/10.3390/biom9100513.

[38] A.A. Gurtovenko, I. Vattulainen, Effect of NaCl and KCl on phosphatidylcholine and phosphatidylethanolamine lipid membranes: insight from atomic-scale simulations for understanding salt-induced effects in the plasma membrane, J. Phys. Chem. B 112 (2008) 1953–1962, https://doi.org/10.1021/jp0750708.

[39] M. Roux, M. Bloom, Ca2+, Mg2+, Li+, Na+, and K+ distributions in the headgroup region of binary membranes of phosphatidylcholine and phosphatidylserine as seen by deuterium NMR, Biochemistry 29 (1990) 7077–7089, https://doi.org/10.1021/bi00482a019.

[40] A. Melcrová, S. Pokorna, S. Pullanchery, M. Kohagen, P. Jurkiewicz, M. Hof, P. Jungwirth, P.S. Cremer, L. Cwiklik, The complex nature of calcium cation

interactions with phospholipid bilayers, Sci. Rep. 6 (2016) 1–12, https://doi.org/10.1038/srep38035.
[41] P. Maity, B. Saha, G.S. Kumar, S. Karmakar, Binding of monovalent alkali metal ions with negatively charged phospholipid membranes, Biochim. Biophys. Acta Biomembr. 1858 (2016) 706–714, https://doi.org/10.1016/j.bbamem.2016.01.012.
[42] B. Rózycki, R. Lipowsky, Spontaneous curvature of bilayer membranes from molecular simulations: asymmetric lipid densities and asymmetric adsorption, J. Chem. Phys. 142 (2015) 1–17, https://doi.org/10.1063/1.4906149.